Fluid mechanics for path planning and obstacle avoidance of mobile robots

Rainer Palm and Dimiter Driankov
AASS, "Orebro University,
SE-70182, "Orebro, Sweden
emails: rub.palm@t-online.de, dimiter.driankov@oru.se

Keywords: Mobile robots, obstacle avoidance, fluid mechanics, velocity potential

Abstract: Obstacle avoidance is an important issue for off-line path planning and on-line reaction to unforeseen appearance of obstacles during motion of a non-holonomic mobile robot along a predefined trajectory. Possible trajectories for obstacle avoidance are modeled by the velocity potential using a uniform flow plus a doublet representing a cylindrical obstacle. In the case of an appearance of an obstacle in the sensor cone of the robot a set of streamlines is computed from which a streamline is selected that guarantees a smooth transition from/to the planned trajectory. To avoid collisions with other robots a combination of velocity potential and force potential and/or the change of streamlines during operation (lane hopping) are discussed.

1 Introduction

Obstacle avoidance is important for off-line planning and on-line reaction to unforeseen and sudden appearance of obstacles during motion of non-holonomic mobile robots. Several methods have been applied to obstacle avoidance in the artificial force potential field method introduced by Khatib in 1985 [1]. The idea is to introduce artificial attractive and repulsive forces that enable the robot to move around an obstacle while aiming at a final target at the same time. Optimization techniques like market-based optimization (MBO) particle swarm optimization (PSO) influencing artificial potential fields have been presented by Palm and Bouguerra [2, 3]. Other approaches have been presented by Borenstein [4], who introduced the vector field histogram technique, and Michels [5] who applied the reinforcement learning method. Specific ad hoc heuristics have been proposed by Fayen [6] and Becker [7].

Despite of the simplicity and elegance of the artificial force potential field method the risk of deadlocks (local minima) or undesired movements in the vicinity of obstacles should be realized. Reinforcement learning may be able to cope with this drawback but to the costs of a high computational effort.

Another kind of artificial potential for obstacle avoidance was therefore introduced by Khosla [8] who used the *velocity potential* of fluid mechanics to construct stream lines in a working area of a mobile robot moving around obstacles in a very natural way. The velocity potential approach is a method which considers both the path/trajectory planning in the case of a well known scenario including static obstacles and the on-line reaction to unplanned situations like obstacle avoidance in an unknown terrain.

Kim and Khosla continued this work with the use of the velocity potential function to avoid obstacles in real time [9]. Further similar research has been published by Li et al [10], Ge et al [11], Waydo and Murray [12], Daily and Bevly [13], Sugiyama [14, 15], Gingras et al [16], and Owen et al [17]. Most of these approaches use a *point source/point sink* combination for flow construction. This can be of disadvantage in the presence of a combination of tracking velocity vectors and obstacle avoidance vectors.

Therefore in this paper the uniform flow of a fluid around an obstacle is preferred. Possible trajectories for obstacle avoidance are modeled by the velocity potential using a uniform flow plus a doublet representing a cylindrical obstacle. The motion of a non-holonomic mobile robot is firstly defined by a predefined trajectory. In the case of an appearance of one or more obstacles in the sensor cone of the robot a set of streamlines is computed from which those streamline is selected that guar-

antees a smooth transition from the planned trajectory to the streamline and, after having left behind the obstacle, back to the original trajectory. To avoid collisions with other moving obstacles (e.g. robots) a combination of velocity potential and force potential is discussed. In the case of possible collisions between robots moving on crossing streamlines a change between streamlines during operation (lane hopping) is presented.

2 Modeling of the system

2.1 Kinematics

We consider a non-holonomic rear-wheel driven vehicle with the kinematics of a car. The kinematic of the non-holonomic vehicle is described by

$$\begin{aligned} \dot{q}_i &= R_i(q_i) \cdot u_i \\ q_i &= (x_i, y_i, \Theta_i, \phi_i)^T \\ R_i(q_i) &= \begin{pmatrix} \cos\Theta_i & 0 \\ \sin\Theta_i & 0 \\ \frac{1}{l_i} \cdot \tan\phi_i & 0 \\ 0 & 1 \end{pmatrix} \end{aligned} \quad (1)$$

where
$q_i \in \Re^4$ - state vector
$u_i = (u_{1i}, u_{2i})^T \in \Re^2$ - control vector, pushing/steering speed
$x_{ip} = (x_i, y_i)^T \in \Re^2$ - position vector of platform P_i
Θ_i - orientation angle
ϕ_i - steering angle
l_i - length of vehicle

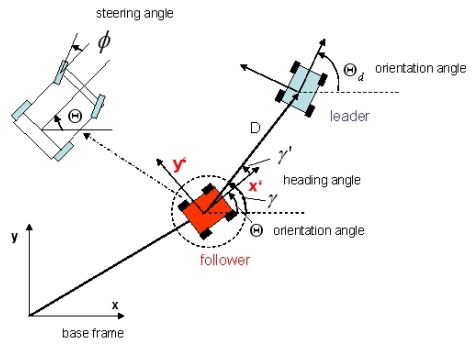

Figure 1: Leader follower principle

2.2 Virtual leader

Many tracking methods use a predefined path or a trajectory as a control reference for the vehicle to be controlled. In contrast to this a 'virtual' vehicle (the leader) is introduced that moves in front of the 'real' vehicle (the follower) (see also [18]). The virtual leader acts as trajectory generator for the real platform at every time step, based on starting and end position (target), obstacles to be avoided, other platforms to be taken into account etc (see Fig. 1). The dynamics of the virtual platform is designed as a first order system that automatically avoids abrupt changes in position and orientation

$$\dot{v}_{vi} = k_{vi}(v_{vi} - v_{di}) \quad (2)$$

$v_{vi} \in \Re^2$ - velocity of virtual platform P_i
$v_{di} \in \Re^2$ - desired velocity of virtual platform P_i
$k_{vi} \in \Re^{2\times 2}$ - damping matrix (diagonal)

v_{di} is composed of the tracking velocity v_{ti} and velocity terms due to artificial potential fields from obstacles and other platforms The tracking velocity is designed as a control term

$$v_{ti} = k_{ti}(p_{xi} - x_{ti}) \quad (3)$$

$x_{ti} \in \Re^2$ - position vector of target T_i
$p_{xi} \in \Re^2$ - position vector of platform P_i
$k_{ti} \in \Re^{2\times 2}$ - gain matrix (diagonal)

There are many ways of computing the control vector u_i for the follower in (1). Under the assumption of a slowly time varying 'leader-follower' system a local linear gain scheduler is applied that is designed according to [19].

3 Some principles of fluid mechanics

A closer look at the problem of path planning and obstacle avoidance leads to a similar case when fluids circumvent obstacles in a smooth and energy saving way. The result is a bundle of trajectories from which one can conclude how an autonomous robot should behave under non-holonomic constraints. In the theory of fluids the terms *velocity potential*, *stream function* and *complex potential* are introduced [20]. The so-called *uniform parallel flow* is introduced that corresponds to an undisturbed trajectory along straight lines. The *flow of a doublet* corresponds to a flow around a cylinder. *Superposition of uniform flow and doublet* leads to a model of a uniform flow around a cylindrical obstacle.

3.1 Superposition of uniform flow and doublet

The flow around a cylindrical object - an obstacle - is finally computed by a superposition of the uniform flow and the doublet which is a superposition of their complex potentials (see Fig. 2).

$$w(z) = U \cdot z + U\frac{r_0^2}{z - z_0} \tag{4}$$

where U is the flow, r_0 is the radius of the obstacle $z = r(cos\Theta + isin\Theta)$ is the complex variable. z_0 is the position of the obstacle in the complex plane, Θ is the angle between z and the imaginary axis (see Fig. 2) The velocity components in polar coordinates are obtained as

$$\begin{aligned} v_r &= U \cdot ((1 + \frac{r_0^2}{z_{re}^2 + z_{im}^2})cos\Theta \\ &- \frac{2z_{re} \cdot r_0^2(z_{re}cos\Theta + z_{im}sin\Theta)}{(z_{re}^2 + z_{im}^2)^2}) \end{aligned} \tag{5}$$

$$\begin{aligned} v_\Theta &= -U \cdot ((1 + \frac{r_0^2}{z_{re}^2 + z_{im}^2})sin\Theta \\ &+ \frac{2z_{re} \cdot r_0^2(-z_{re}sin\Theta + z_{im}cos\Theta)}{(z_{re}^2 + z_{im}^2)^2}) \end{aligned} \tag{6}$$

where $z_{re} = rcos\Theta - x_0$ and $z_{im} = rsin\Theta - y_0$. Here one has to mention that stream lines not only exist outside but also inside the cylinder. The speciality of this flow model is that the surface of the cylinder itself is a streamline. Therefore one can ignore the stream lines inside the cylinder because the surface of the cylinder serves as a borderline for stream lines that cannot be trespassed.

3.2 Superposition of two or more cylinders

For more than one cylinder weighting functions μ_i for the flows U_i are introduced depending on the distance of the actual robot position d_i to the cylinder surfaces [12, 13]

$$\mu_i = \prod_{i \neq j} \frac{d_j}{d_i + d_j}; \quad U_i = \mu_i \cdot U \tag{7}$$

From (5), (6), and (7) one obtains velocity components v_{ri} and $v_{\Theta i}$ in polar coordinates that will be transformed into cartesian coordinates by

$$(u_i, v_i)^T = \begin{pmatrix} cos(\Theta) & -sin(\Theta) \\ sin(\Theta) & cos(\Theta) \end{pmatrix} \cdot (v_{ri}, v_{\Theta i})^T \tag{8}$$

Summerizing the velocities u_i in x-direction and v_i in y-direction in cartesian coordinates

$$u_{tot} = \sum_i u_i \quad v_{tot} = \sum_i v_i \tag{9}$$

leads to the streamlines for the multiple obstacle case.

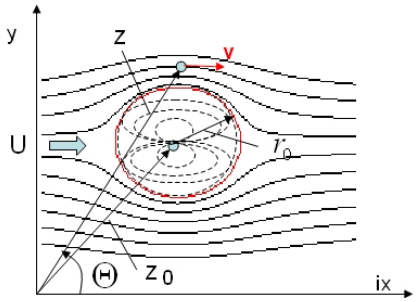

Figure 2: Flow around a cylinder

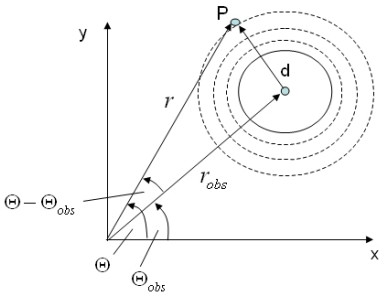

Figure 3: Force potential

3.3 Comparison between velocity and force potential

In the following a comparison between velocity and force potential shows the contrasts and the similarities between these two types of potentials. The force potential of a circular object (see Fig. 3) is given by

$$p_{force} = \frac{c}{d} \tag{10}$$

with c - strength of potential field
$d = \sqrt{r^2 - 2rr_{obs}cos(\Theta - \Theta_{obs}) + r_{obs}^2}$

For a point $P(r, \Theta)$ the repulsive force and - with this - the repulsive velocity $v_{rep} = (v_r, v_\Theta)^T$ yields

$$v_r = \frac{dp}{dr} = -\frac{c}{d^2} \cdot \frac{r - r_{obs} \cdot cos(\Theta - \Theta_{obs})}{d} \tag{11}$$

$$v_\Theta = \frac{dp}{r \cdot d\Theta} = -\frac{c}{d^2} \cdot \frac{r_{obs} \cdot sin(\Theta - \Theta_{obs})}{d} \tag{12}$$

Compared with the flow of a doublet and the corresponding velocities (5) and (6) we can conclude

that these two concepts are different but also have common features: after some conversions the force potential appears as a term in the velocity potential. A crucial point, however, is that for the force potential the "streamlines" always point in the direction away from the "gravity center". By contrast for the velocity potential field the stream lines Ψ always have a tangential component This is of great advantage for obstacle avoidance because it helps a mobile vehicle to move around the obstacle in an optimal way in the sense that the streamlines are symmetrical with respect to the axis perpendicular to the flow going through the "poles" of the cylinder. However a combination of velocity and force potential should also be considered. Such a combination takes place if during tracking along a streamline an unforeseen moving obstacle - e.g. another robot - appears in the sensor cone. In this case the current trajectory given by the actual streamline is corrected by the repulsive force of the moving obstacle.

4 Obstacle avoidance using the velocity potential

The previous calculations of the velocity potential are performed in a coordinate frame corresponding to the local robot frame. In the multi-robot case this concerns every involved robot so that a total view of the whole scenario can only be obtained from the viewpoint of the base frame.

Figure 4 shows the relationship between the robot frame T1 and the base frame T0. The transformation matrix between T1 and T0 is

$$A_{10} = \begin{pmatrix} cos(\alpha) & -sin(\alpha) & x_d \\ sin(\alpha) & cos(\alpha) & y_d \\ 0 & 0 & 1 \end{pmatrix} \qquad (13)$$

To compute the streamline array $v_{flow,rob} = (v_r, v_\Theta, 1)^T$ in the base frame the following steps are necessary:

1. Transform the obstacle coordinates into the robot frame
$$p_{obs,rob} = A_{10}^{-1} \cdot p_{obs,base} \qquad (14)$$
2. Calculate the streamline arrays $v_{flow,rob}(k)$, k - discrete time step, from eqs. (5) and (6) in T1 and the corresponding flow trajectory $p_{flow,rob}(k)$ of the flow.
3. Transform the flow trajectory $p_{flow,rob}$ into the base frame T0
$$p_{flow,base}(k) = A_{10} \cdot p_{flow,rob}(k) \qquad (15)$$

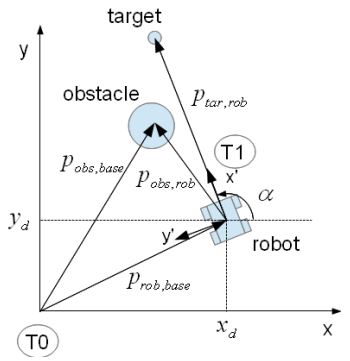

Figure 4: Relations between frames

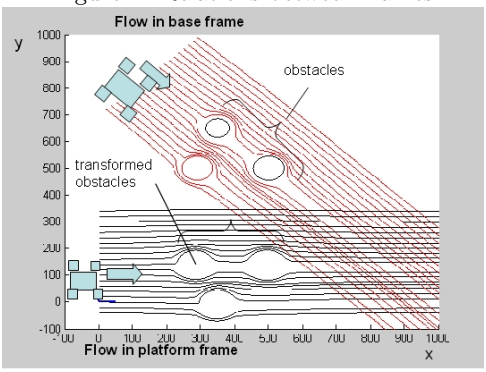

Figure 5: Transformation between frames

Figure 5 shows the particular stages of the computation of stream lines.

Remark: A stagnation point near the obstacle should be recognized in a very early stage. A corresponding test is relatively simple and is to be done in the robot frame for every streamline: Check the x-coordinate x_{endi} of the endpoint of streamline i relative to the x-coordinate x_{obs} of the obstacle. If $x_{endi} \leq x_{obs}$ then the regarding streamline ends up with a stagnation point and should be excluded. A more conservative test is $x_{endi} \leq x_{obs} + C$, where C is a positive number, e.g. $C = 2 \cdot r_0$

After that, those streamline is selected for the robot which lies closest to the original predefined trajectory. In order to get a smooth connection to the original trajectory the following transition filter is used

$$p_x(k+1) = p_x(k) + K_{filt} \cdot (x_{array}(k+1) - p_x(k)) \qquad (16)$$

where $p_x(k) \in \Re^2$ - actual position of robot, $x_{array}(k) = p_{flow,base}(k)$, $K_{filt} \in \Re^{2\times 2}$ - filter matrix.

For the change from a streamline to the original trajectory we have to consider two cases:

1. A trajectory $x_{traj}(k)$ is defined between start-

ing point $x_{traj}(1)$ and endpoint $x_{traj}(k_{end})$.
2. Only the target endpoint x_{traj} plus constraints upon the velocities $v = (u, v)^T$ are defined.
Case 1 is difficult to solve because the original trajectory is cut into 3 parts: a part before entering the streamlines with $k = 1...k_{in}$, a part which is covered by the area of streamlines with $k = k_{in}...k_{tr,out}$, and a part with $k = k_{tr,out}...k_{end}$ after the area of streamlines. Suppose that the trajectory leaves the area of streamlines between two endpoints of streamlines. $x_{traj}(k_{in})$ be the point on the trajectory at k_{in} when the robot (and the trajectory) enters the area of streamlines. $x_{traj}(k_{tr,out})$ is the point on the trajectory at $k_{tr,out}$ when the trajectory leaves the area of streamlines. $x_{traj}(k_{end})$ is the end of the trajectory at k_{end}. At first one has to search for the first trajectory point $x_{traj}(k_{tr,out})$ after having left the area of streamlines (see Fig. 6). A solution to this is the following:
1. Transform the total trajectory $x_{traj}(k)$ into the robot frame T1

$$x_{traj_{rob}}(k) = A_{01}(k_{out}) \cdot x_{traj}(k) \qquad (17)$$
$$A_{01} = A_{10}^{-1}; \quad k = 1...k_{end}$$

where k_{out} is the time point for the robot to leave the area of streamlines.

2. Search for the first trajectory point for which $x_{traj_{rob}}(k) > 0$; $k > k_{in}$. The result is $x_{traj_{rob}}(k_{tr,out})$. Choose another trajectory point $x_{traj_{rob}}(k_{tr,out_1}) > x_{traj_{rob}}(k_{tr,out})$; $k_{tr,out_1} > k_{tr,out}$ to enable a smoother transition.

3. Activate a transition filter

$$p_x(k+1) = \qquad (18)$$
$$p_x(k) + K_{filt} \cdot (x_{traj}(k_{tr,out_1} + k) - p_x(k))$$

where $k = 1...(k_{end} - k_{tr,out_1})$, which guarantees a smooth transition to the original trajectory.

Case 2 is simpler: once having left a streamline it is immediately possible for the robot to move to the target x_{traj}. We introduce another transition filter which guarantees a smooth transition between a streamline and the target. Let $p_x(k_{out})$ be the position of the robot at the end of the streamline. Then we obtain for the transition filter

$$p_x(k+1) = p_x(k) + K_{filt} \cdot (x_{traj}(k_{end}) - p_x(k)) \qquad (19)$$

where $k \geq k_{out}$.

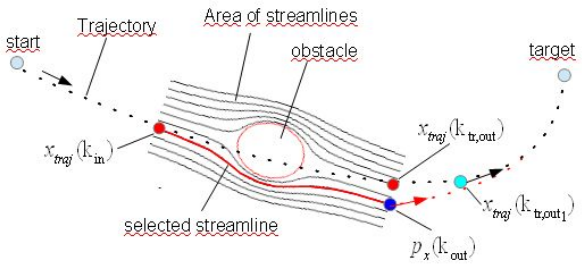

Figure 6: Transition between trajectory and streamline

5 Changing of streamlines during operation (lane hopping)

First of all it has to be stressed that the change of a streamline during operation (lane hopping) becomes feasible if several streamlines are computed in advance. Each streamline constitutes a possible trajectory for the mobile platform. Once a streamline is selected for a platform it may be necessary to leave the actual streamline (lane) during operation and change to another one because of the following reasons:

1. The platform is too close to a static obstacle
2. The streamline violates hard/soft constraints
3. The platform is expected to collide with another moving obstacle (platform)

Lane hopping means the change from the current streamline to another streamline which may be a neighboring streamline but not necessarily. Figure 7 presents a case where the robot changes the streamlines to avoid a motion too close to the obstacles. This change should not be too abrupt but rather a smooth transition (see Fig. 8). This is again realized by a filter function either in the robot or world frame

$$dx_{fluid}(k+1) =$$
$$K_{filt} \cdot (x_{array}(k+1|lane_{new}) - p_x(k)) \qquad (20)$$
$$p_x(k+1) = p_x(k) + dx_{fluid}(k+1)$$

where it is assumed that the x-positions in the robot frame $x_{array}(k|lane_{old}) \approx x_{array}(k|lane_{new})$. If $x_{array}(k|lane_{old}) > x_{array}(k|lane_{new})$ then (20) has to be corrected to

$$dx_{fluid}(k+1) = K_{filt} \cdot (x_{array}(k+\delta|lane_{new}) - p_x(k)) \qquad (21)$$

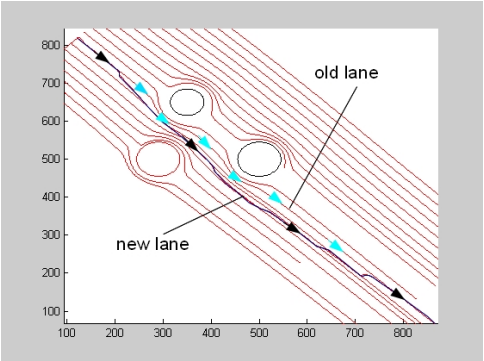

Figure 7: Change of streamline (lane hopping)

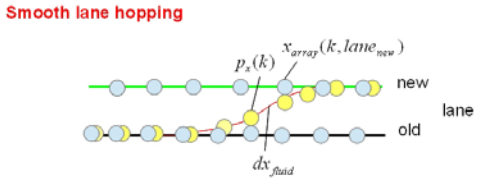

Figure 8: Principle of lane hopping

δ is the number of time steps for which

$$x_{array}(k|lane_{old}) \approx x_{array}(k+\delta|lane_{new}) \quad (22)$$

In the case of a global (centralized) control of the robot fleet it is possible to compute possible collisions of platforms in advance if they would keep on moving on the originally chosen lanes. Let us compare the 5 lanes each of platforms 1 and 2 and calculate the discrete time stamps at their crossings, and the difference between these time stamps. Let for example robot 1 move on lane 5 and robot 2 on lane 2. Lanes 5 and 2 cross at $t = 367$ for robot 1 (see Fig. 9, matrix K12, blue circle) and for robot 2 at $t = 369$ (see matrix J12, blue circle) . The distance between the two entries is 2 (see Fig. 9, matrix del12) which points to a collision at time $t \approx 367$. In order to avoid a collision many different options are possible. We have chosen the following option: robot 1 $\rightarrow$ lane 4, robot 2 $\rightarrow$ lane 1. The result can also be observed in Fig. 9, red circles. The difference (distance) between the time stamps $t = 316$ for robot 1 and $t = 366$ for robot 2 is 50 which is sufficient for avoiding a collision. See also Figs. 14 and 15

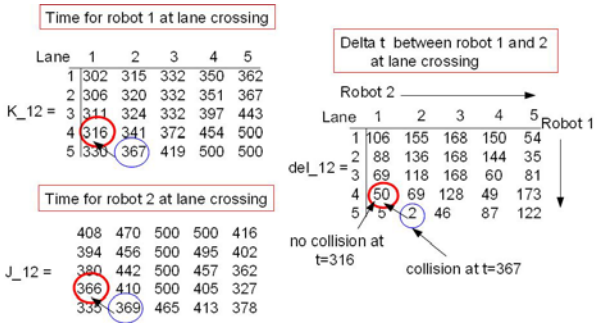

Figure 9: Simulation example, with/without lane hopping

6 Simulation results

The simulation shows 3 mobile robots (platforms) aiming at their targets (see Fig. 10), crossing areas of 3 obstacles while sharing a common working area for some time. Platform p2 switches on first its streamline because obstacle O1 is first detected. Then follows p3 seeing O3 in its sensor cone and finally p1 with O1 in its sensor cone (see Fig. 11). Then the platforms 'switch off' their streamlines in the sequence p1, p3, p2 (because the obstacles disappear from their sensor cones) and reach finally their targets (see Fig. 12). The final trajectories show the interplay of different influences from planned trajectories, streamlines, and artificial force fields in the case when robots avoid each other. Figure 13 shows the regarding velocity profiles of the individual robots and the switching sequence of the streamlines.

As to the change of streamlines (lane hopping) the imminent danger of a collision between robots 1 and 2 is shown in Fig. 15. Figure 15 shows that lane hopping avoids a collision between robots 1 and 2 provided that the change of the lanes takes place in a sufficient distance to the possible collision. A practical solution is the following:

- Check the time t_{cross} to a possible collision
- Calculate the time t_{change} to change between two neighboring lanes
- Start changing at least $2 \cdot t_{change}$ before possible crossing

If it is not sufficient to change to a neighboring lane then apply the same procedure to another lane while taking into account longer changing times because of the longer distance between the lanes.

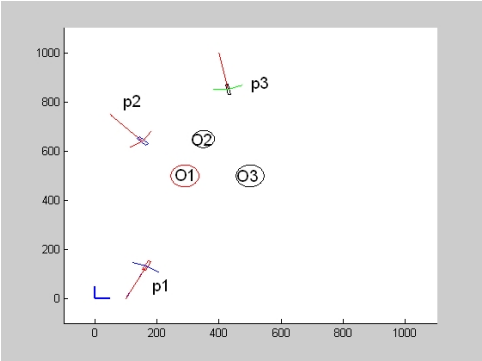

Figure 10: No stream lines on

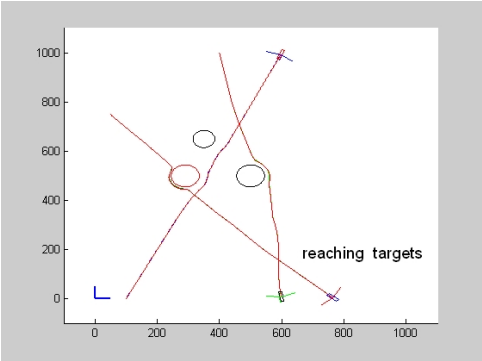

Figure 12: Platforms reach targets

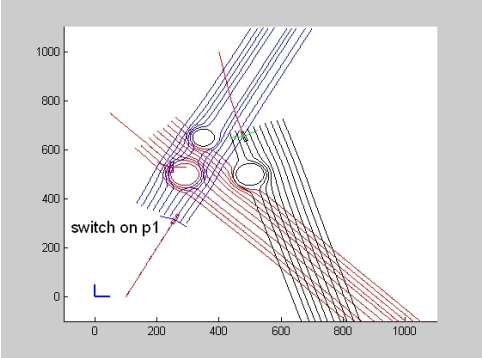

Figure 11: All platforms streamlines on

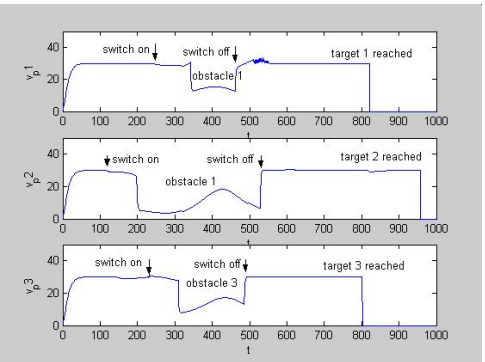

Figure 13: Velocity profiles

7 Conclusions

Fluid mechanics and its velocity potential principle is a powerful mean both for path planning and sensor guided on-line reaction to obstacles. The velocity potential has been used for avoiding static obstacles together with the force potential for moving obstacles. Finally it has been shown that the change of streamlines during operation can avoid imminent collisions between robots. This change is done in a smooth way and at an early stage before a possible collision. To avoid possible collisions between robots moving on crossing streamlines a change between streamlines during operation (lane hopping) is presented. A critical aspect is that obstacles are very rarely cylindrical. This, however, can easily be handled by a rough approximation of the obstacle by an appropriate number of cylinders. The driveable streamlines are then lying at the edges (left or right) of the conglomerate of cylinders [13]. The computational effort of the method is mainly determined by equations (5, 6, 8, 14, 15) computed for n streamlines and m time steps but only at the moment of the detection of an obstacle. A future work lies therefore in the modeling of the stream lines to make the use of the approach easier for real applications.

References

[1] O. Khatib. Real-time 0bstacle avoidance for manipulators and mobile robots. *IEEE Int. Conf. On Robotics and Automation,St. Loius,Missouri, 1985*, page 500505, 1985.

[2] R.Palm and A. Bouguerra. Navigation of mobile robots by potential field methods and market-based optimization. *ECMR 2011*, Oerebro, Sweden., 2011.

[3] R. Palm and A. Bouguerra. Particle swarm optimization of potential fields for obstacle avoidance. In *Proceeding of RARM 2013, Istanbul, Turkey.* Volume: Scient. coop. Intern. Conf. in elect. and electr. eng., Sept. 2013.

[4] J. Borenstein and Y. Koren. The vector field histogram - fast obstacle avoidance for mobile robots. *IEEE Trans. on Robotics and Automation, Vol. 7, No 3*, pages 278–288, June 1991.

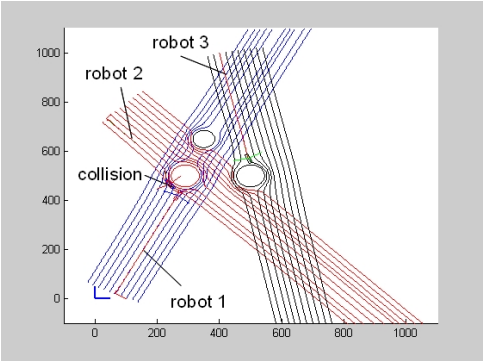

Figure 14: Simulation example, no lane hopping

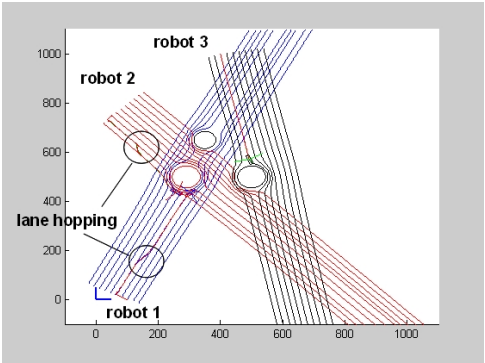

Figure 15: Simulation example, with lane hopping

[5] J. Michels, A. Saxena, and A. Y. Ng. High speed obstacle avoidance using monocular vision and reinforcement learning. *22nd Int'l Conf on Machine Learning (ICML), Bonn, Germany*, 2005.

[6] B.R.Fayen and W.H.Warren. A dynamical model of visually-guided steering, obstacle avoidance, and route selection. *International Journal of Computer Vision, 54(1/2/3)*, page 1334, 2003.

[7] M. Becker, C. Dantas, and W. Macedo. Obstacle avoidance procedure for mobile robots. In *ABCM Symposium in Mechatronics, vol. 2*. ABCM, 2006.

[8] P. K. Khosla and R. Volpe. Superquadric avoidance potentials for obstacle avoidance. In *IEEE Conference on Robotics and Automation, Philadelphia PA*. IEEE, Springer-Verlag London, April 1988.

[9] Jin-Oh Kim and P. K. Khosla. Real-time obstacle avoidance using harmonic potential functions. *IEEE Trans on Robotics and Automation,*, pages 1–27, 1992.

[10] Z. X. Li and T. D. Bui. Robot path planning using fluid model. *Journal of Intelligent and Robotic Systems, vol. 21*, pages 29–50, 1998.

[11] S.S. Ge and Y.J. Cui. Dynamic motion planning for mobile robots using potential field method. *Autonomous Robots, 13*, pages 207 – 222, 2002.

[12] S. Waydo and R. M. Murray. Vehicle motion planning using stream functions. In *Proc. IEEE Int. Conf. Rob. Autom., volume 2*. IEEE, 2003.

[13] R. Daily and D. M. Bevly. Harmonic potential field path planning for high speed vehicles. *American Control Conference, 2008, Seattle, Washington, USA*, pages 4609 – 4614, 2008.

[14] S. Sugiyama and S. Akishita. Path planning for mobile robot at a crossroads by using hydrodynamic potential. In *Proc. of 1998 JAPAN-U.S.A SYMPOSIUM ON FLEXIBLE AUTOMATION*, 1998.

[15] S. Sugiyama, J. Yamada, and T. Yoshikawa. Path planning of a mobile robot for avoiding moving obstacles with improved velocity control by using the hydrodynamic potential. *IEEE/RSJ Intern. Conf. on Intell. Robots and Systems*, page 207222, 2010.

[16] D. Gingras, E. Dupuis, G. Payre, and J. Lafontaine. Path planning based on fluid mechanics for mobile robots using unstructured terrain models. In *Proceedings ICRA 2010*. ICRA 2010, 2010.

[17] T. Owen, R. Hillier, and D. Lau. Smooth path planning around elliptical obstacles using potential flow for non-holomonic robots. In *Robocup 2011: Soccer World Cup XV, volume 7416*, 2011.

[18] N. E. Leonard and E. Fiorelli. Virtual leaders, artificial potentials and coordinated control of groups. *Proc. of the 40th IEEE Conf. on Decision and Control, Orlanda, Florida USA*, pages 2968–2973, Dec 2001.

[19] R. Palm and A. Bouguerra. Particle swarm optimization of potential fields for obstacle avoidance. In *Proc. of RARM 2013, Istanbul 09/2013*, Sept. 2013.

[20] Y. Nakayama. Introduction to fluid mechanics. *Butterworth-Heinemann, Oxford Auckland Boston*, 1999.